Object Detection in Biosonar Based Robot Navigation

Majid M. Beigi and Andreas Zell

***Abstract*— This paper addresses the problem of object detection in a biosonar based mobile robot in a natural environment. In our previous work [9] we presented a time resolved spectrum kernel to extract the similarities between subsequences of the echoes reflected by different trees and we could get higher accuracy than methods which used specific features in all echoes. In this paper we present a more general kernel called *warped time-resolved spectrum kernel* which considers warping in the subsequences. Furthermore, having a set of those kernels for different size of subsequences, we find the optimal kernel selection via maximizing the Kernel Fisher Discriminant criterion (KFD) to build the optimal linear combination of kernels. We compare the obtained results with our previous work.**

I. INTRODUCTION

Bats can distinguish objects and their prey by emitting a series of ultrasound signals (chirps) that generally sweep covering frequencies from 22 to 100 kHz. They can separately perceive the delays of two concurrent echoes as little as 2 ms apart and resolve reflecting points as close together as 0.3 mm in range [5]. The acoustic image of a sonar target is apparently derived from time-domain or periodicity information processing by the nervous system. Inspired by the bat biosonar system, researchers have utilized ultrasonic sensing techniques for mobile robots (biomimetic robots) and tried to classify different textures and landmarks using received echo signals. Biosonar sensing involves the production of chirps, the reception of echoes from targets, signal analysis and target matching. By comparing the returning echoes (which are individually the superposition results of the reflected echoes) we aim at recognizing the objects. Gao et. al [6] presented a deformable template matching algorithm for classification of several types of brick walls, picket fences and hedges using sonar echoes. M. Wang et al. [8], [7] used different structural features in the frequency domain and also cross correlation as template matching algorithm for that task. In our previous work [9] we suggested a kernel named *Time-resolved spectrum kernel* for matching the subsequences of time series (sonar echoes) and extracting the local similarities of echoes. The results outperformed other matching techniques [8], [7]. The time-resolved spectrum kernel simply measures the whole similarities of all subsequences of the time series in consideration, without considering warping and independent of their positions. The more two time series share similar subsequences, the more similar they are. A linear combination of kernels with different subsequence size (p-spectrum kernels) was a measure of similarity between two time series. In this paper we present a more general kernel called *warped time-resolved spectrum kernel*, which also considers all possible warpings in subsequences. Furthermore, having a set of those kernels, we find the optimal kernel selection via maximizing the Kernel Fisher Discriminant criterion (KFD) to build the optimal linear combination of kernels. We compare the obtained results with our previous works.

M. M. Beigi is PhD. student at the Department of Computer Science, University of Tuebingen, D72076, Germany. majid.beigi@uni-tuebingen.de

A. Zell is Professor at the Department of Computer Science, University of Tuebingen, D72076, Germany. Andreas.Zell@uni-tuebingen.de

II. BIOSONAR BASED ROBOT

A. Hardware

The implementation of the whole system consists of a mobile robot (Robin) with two PCs, a digital signal processing package, and a biosonar system (Fig. 1). The biosonar system includes a National Instruments NI6110 analog I/O card, a mini servo controller (module SSCII), a BNC2110 connector, and the biosonar head. The NI6110 card and the BNC2110 connector transfer chirp signals and receive the reflected echoes. The biosonar head (Fig. 2) consists of 3 Polaroid sensors in a triangular layout, similar to the layout of a bat's mouth and ears: two Polaroid 600 sensors spaced 12.5 cm apart as *ears*, a Polaroid 7000 sensor as *mouth* in the middle between two ears. Each of the two ears has two degrees of angular freedom provided by two servo motors. These can be finely rotated to acquire local support. The Polaroid ultrasonic ranging system is most commonly used by the robotics research community. The emitted pulse was a linearly frequency modulated chirp sweeping from 20kHz to 120kHz in 1 ms (Fig.2). The maximum sampling speed of the NI6110 card is 5 MHz. We utilized 1 MHz in our research. The NiMH charger box provides the sensors with a 150V power supply. The mobile robot Robin is an autonomous mobile service robot that has two PCs inside, one is in charge of navigation control, the other one is responsible for signal data processing, feature extraction and decision making.

B. Landmarks and sensing strategy

Through echolocation in darkness, a bat can perceive not only the position of an object, but also its 3D structure [1]. The recognizable target in nature works as a landmark for its navigation. For our sensory task – biosonar based mobile robot navigation in natural environments – these landmarks should be rich and easy to be found there. The criteria for selecting natural landmarks include observability, frequent occurrence, uniqueness, temporal stability, easy classification, and lateral compactness [2]. Considering those aspects,

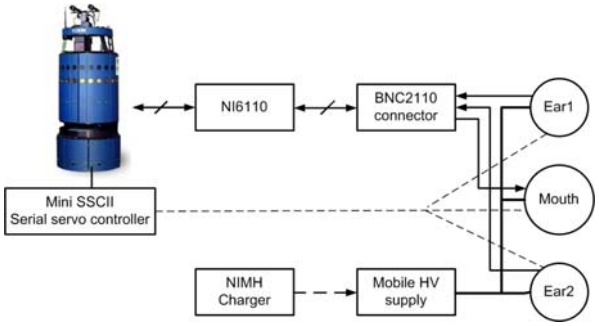

Fig. 1. Biosonar system configuration

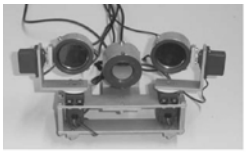

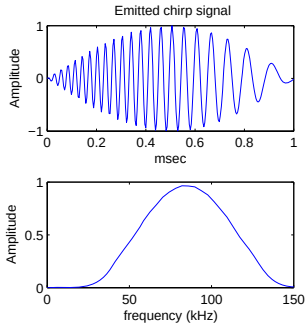

Fig. 2. Biosonar head (left). Emitted chirp signal and its frequency content (right).

we selected three artificial trees with similar height of 1.7 m as shown in Fig. 3.

Compared with other researchers [3], [4], we used a different method for sensing the objects. We used a 0.5 degree angular stepsize for our scans, each tree was scanned 360 degrees in a circular movement of the robot and we collected echoes from all orientations of leaves and tree. The reflected echo contains the information about the geometry of the tree and is the superposition of all reflections.

C. data processing

Fig. 4 shows the block diagram of the data acquisition and preprocessing procedure of reflected echoes. We passed the reflected echoes through a bank of 10 gammatone filters between 20 kHz and 120 kHz. In order to extract the envelope of the filtered signals, they were delivered to half-wave rectifiers.

The next step is *frame blocking*. In this step the signal

Fig. 3. Three different trees as biosonar landmarks. From left to right: Ficus, Bamboo, Schefflera.

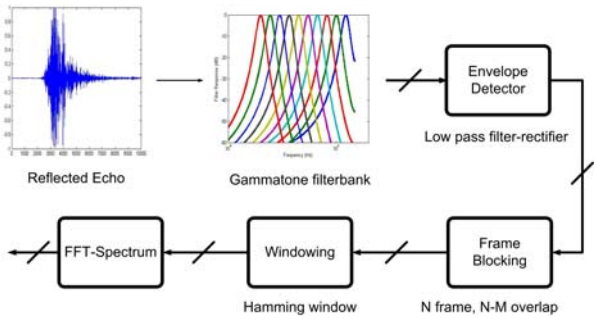

Fig. 4. Block diagram of the preprocessing steps for reflected echoes.

blocked to frames of N samples, is separated from adjacent frames by M $(M < N)$ samples and has $N - M$ overlaps. Considering the sampling frequency of the data acquisition part (1 MHz) and the minimum width of leaves of trees and axial resolution of transducers, we selected $N = 32$ and 50% overlap for frames. The next step in the data preprocessing is to window each individual frame so as to minimize the signal discontinuities at the beginning and end of each frame. We used a *Hamming window* for this purpose. The last step is to calculate the average energy of each band of gammatone filter bank in each frame. The result is a feature matrix, where each column is a vector showing the average energy of each channel in one time frame. Fig. 5 shows the examples of the preprocessed echoes of Ficus and Schefflera trees. We use this feature matrix for our classification task.

As noted before, the problem is that the biosonar signals are random and nonstationary in the temporal dimension. For example, the location of leaves in the plant determines the acoustic energy throughout the frames, and small changes in the orientation of the plant result in changes in those features along the frames of time. But, as we see in Fig. 5, despite the randomness of those signals there are some local similarities (shown by p) in echoes from one tree. Then, if we can find the sizes of windows in which we have maximum similarity between data of one object it can help us to classify that object from others. We consider the output of the block diagram shown in Fig. 4, a time series in which each point is a time frame and its value is a vector of features (the average energy of each channel of gammatone filter bank). We should find the subsequences of the time series *independent of the positions of occurrences* that have maximum similarities in echoes of each object. The intuition behind our idea is that the structure of objects and, as an example, the size of leaves or branches, should be considered in the classification task. The size of the subsequence that we are looking for can be related to the size of the leaves or branches of the tree. In another way, the energy reflected by the leaves or branches of the tree can be related to the size of those similar subsequences of the time series.

III. Algorithms

A kernel function can often be considered as a measure of similarity. Different kernels correspond to different notions

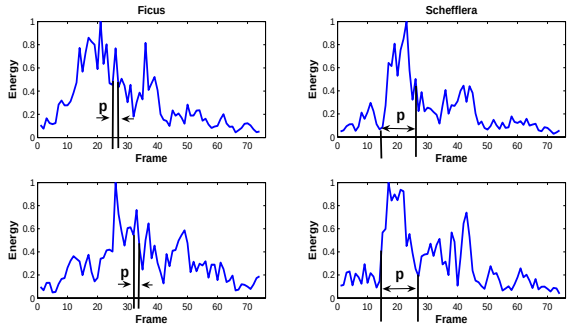

Fig. 5. The energy spectrum in each time frame for Ficus and Schefflera trees (output of gammatone filter centered around 50 kHz). The time-resolved spectrum kernel tries to find the local similarities in window of size p in echoes of one object.

of similarity. The use of a kernel makes it possible to perform the mapping into that feature space and to calculate the inner product between those maps. But the main task here is to find a map ϕ that reflects the suitable and common features of those time series and gives a good indication of the similarity we would like to capture. The warped time-resolved spectrum kernel simply measures the whole similarities of all warped non contiguous subsequences of the two time series , independent of their positions. The more two time series share similar subsequences, the more similar they are.

A. Warped time resolved spectrum kernel

A time sequence $s = s_1 ... s_n$ is a sequence of data points at successive times with $s_i \in \Re^d$, where $1 \leq i \leq n$ and d is the dimension of data points. We denote $|s|$ the length of s, $s(i-p+1:i)$ the p-length subsequence of s from position $i-p+1$ to position i, $\mathbf{I}_p^{|s|}$ the set of indices defining all the p-long (*contiguous* or *non-contiguous*) subsequence of s: $\mathbf{I}_p^s = \{\mathbf{i} : \mathbf{i} \in \mathrm{N}^p, 1 \leq i_1 < ... < i_p \leq |s|\}$ and $u = s_{\mathbf{i}}$ as a subsequence of s in positions given by $\mathbf{i} = (i_1, ..., i_{|u|})$. The number of gaps in the subsequence is $g_{\mathbf{i}} = (i_{|u|} - i_1 + 1) - |\mathbf{i}|$. For example, if we consider $s = s_1 s_2 s_3 s_4 s_5$, $u = s_1 s_3 s_5$ is a subsequence of s in the positions $\mathbf{i} = (1, 3, 5)$ of length $|\mathbf{i}| = 3$ and $g_{\mathbf{i}} = 2$.

For $u \in \Sigma^{p \times d}$, the infinite set of all subsequences with size p and dimension d, the implicit embedding map ϕ brings s to a vector space F ($\phi : s \rightarrow (\phi_u(s)) \in F$) and the u component of our feature vector is:

$$\phi_u^p(s) = \sum_{\mathbf{i} \in \mathbf{I}_p^{|s|},\ u \in \Sigma^{p \times d}} \varphi_u(s_{\mathbf{i}}) \gamma^{g_{\mathbf{i}}}$$

where $\gamma \in (0, 1)$ is a decay factor as a cost for warping (non-contiguousity) in the time series and φ is an implicit map that satisfies:

$$\kappa_p(s_{\mathbf{i}}, t_{\mathbf{j}}) = < \varphi_u(s_{\mathbf{i}}),\ \varphi_u(t_{\mathbf{j}}) > \qquad \mathbf{i} \in \mathbf{I}_p^s,\ \mathbf{j} \in \mathbf{I}_p^t,\ u \in \Sigma^{p \times d} \tag{1}$$

in which κ_p is a kernel function that measures the local similarity between two p-length subsequences $s_{\mathbf{i}}$ and $t_{\mathbf{j}}$ of the time series in consideration. In words, $\phi_u^p(s)$ is a sum over all similarities between p-long subsequences of s and u. The dot product of those feature vectors represents the *warped-time resolved p-spectrum kernel*:

$$\begin{aligned}
\mathcal{K}_p(s,t) &= \langle \phi_u^p(s), \phi_u^p(t) \rangle = \textstyle\int_{\mathbf{R}^{d \times p}} \phi_u^p(s) \phi_u^p(t) du \\
&= \sum_{\mathbf{i} \in \mathbf{I}_p^s} \sum_{\mathbf{j} \in \mathbf{I}_p^t} \gamma^{g_{\mathbf{i}}} \gamma^{g_{\mathbf{j}}} \textstyle\int_{R^{d \times p}} \varphi_u(s_{\mathbf{i}}) \varphi_u(t_{\mathbf{j}}) du \\
&= \sum_{\mathbf{i} \in \mathbf{I}_p^s} \sum_{\mathbf{j} \in \mathbf{I}_p^t} \kappa_p(s_{\mathbf{i}}, t_{\mathbf{j}}) \gamma^{g_{\mathbf{i}} + g_{\mathbf{j}}}
\end{aligned}$$

As we see from the above equation, the kernel adds all similarity scores between subsequences, considering all possible degrees of warping. Needless to say, the calculation of that kernel has a very high computational cost. We use dynamic programming to calculate it in an efficient manner and justifiable time.

Considering the definitions of $\mathbf{I}_p^s$ and $\mathbf{I}_p^t$, we express the kernel using a suffix version of that:

$$\mathcal{K}_p(s,t) = \sum_{i=1}^{|s|} \sum_{j=1}^{|t|} \sum_{(\mathbf{i},\mathbf{j}) \in \mathbf{I}_p^{s(1:i)} \times I_p^{t(1:j)}} \kappa_p(s_{\mathbf{i}}, t_{\mathbf{j}}) \gamma^{g_{\mathbf{i}} + g_{\mathbf{j}}}$$

Considering the suffix kernel as:

$$\mathcal{K}_p^S(s(1:i), t(1:j)) = \sum_{(\mathbf{i},\mathbf{j}) \in \mathbf{I}_p^{s(1:i)} \times \mathbf{I}_p^{t(1:j)}} \kappa_p(s_{\mathbf{i}}, t_{\mathbf{j}}) \gamma^{g_{\mathbf{i}} + g_{\mathbf{j}}} \tag{2}$$

we have:

$$\mathcal{K}_p(s,t) = \sum_{i=1}^{|s|} \sum_{j=1}^{|t|} \mathcal{K}_p^S(s(1:i), t(1:j)) \tag{3}$$

We consider $s' = s(1:|s'|)$, $t' = t(1:|t'|)$, $1 \leq |s'| \leq |s|$ and $1 \leq |t'| \leq |t|$ (prefixes of s and t). If we add a new data point x to the time series s', using the above equation we can calculate $\mathcal{K}_p(s'x, t')$:

$$\begin{aligned}
\mathcal{K}_p(s'x, t') &= \sum_{i=1}^{|s'x|} \sum_{j=1}^{|t'|} \mathcal{K}_p^S(s'x(1:i), t'(1:j)) \\
&= \sum_{i=1}^{|s'|} \sum_{j=1}^{|t'|} \mathcal{K}_p^S(s'(1:i), t'(1:j)) + \sum_{j=1}^{|t'|} \mathcal{K}_p^S(s'x, t'(1:j))
\end{aligned}$$

Then,

$$\mathcal{K}_p(s'x, t') = \mathcal{K}_p(s', t') + \sum_{j=1}^{|t'|} \mathcal{K}_p^S(s'x, t'(1:j)) \tag{4}$$

We accept a constraint on choosing the kernel function $\kappa_p(s_{\mathbf{i}}, t_{\mathbf{j}})$ (Equation 1), we suppose:

$$\kappa_p(s_{\mathbf{i}}, t_{\mathbf{j}}) = \textstyle\prod_{i=1}^{p} \kappa^*(s_{\mathbf{i}i}, t_{\mathbf{j}_i})$$

in which κ^* is an arbitrary function that measures the similarity between two data points of the time series. In this study, as a suitable and arbitrary selection we consider $\kappa^*(s_{\mathbf{i}i}, t_{\mathbf{j}_i}) = \exp \frac{-(s_{\mathbf{i}_i} - t_{\mathbf{j}_i})^2}{2\sigma^2}$ to measure the similarity between two data

points, then:

$$\kappa_p(s_{\mathbf{i}}, t_{\mathbf{j}}) = \prod_{i=1}^{p} \kappa^*(s_{\mathbf{i}i}, t_{\mathbf{j}_i}) = \exp\left(-\frac{||s_{\mathbf{i}} - t_{\mathbf{j}}||^2}{2\sigma^2}\right) \quad (5)$$

That, $\kappa_p(s_{\mathbf{i}}, t_{\mathbf{j}})$ is a gaussian kernel of width σ and suitable for measuring the local similarity of subsequences in time series. Then, if we add another new data point y to the time series t', considering the assumption for κ_p and the above definition of $\mathcal{K}_p^S$ (Equation 2), it can be shown:

$$\mathcal{K}_p^S(s'x, t'y) = \kappa^*(x, y) \sum_{i=1}^{|s'|} \sum_{j=1}^{|t'|} \gamma^{|s'|-i+|t'|-j} \mathcal{K}_{p-1}^S(s'(1:i), t'(1:j)) \quad (6)$$

It means when new points are added, to measure the new p-suffix kernel, we must calculate similarities of $p-1$ length subsequences in the suffixes considering all possible degree of warping. To evaluate $\mathcal{K}_p^S$ recursively, we define:

$$\mathcal{K}_p^{Sw}(k, l) = \sum_{i=1}^{k} \sum_{j=1}^{l} \gamma^{k-i+l-j} \mathcal{K}_{p-1}^S(s'(1:i), t'(1:j))$$

Then equation 6 becomes:

$$\mathcal{K}_p^S(s'x, t'y) = \kappa^*(x, y) \mathcal{K}_p^{Sw}(|s'|, |t'|) \quad (7)$$

to express the above kernel recursively, we use the relation:

$$\sum_{i=1}^{a} \sum_{j=1}^{b} f(i,j) = f(a,b) + \sum_{i=1}^{a-1} \sum_{j=1}^{b} f(i,j) + \sum_{i=1}^{a} \sum_{j=1}^{b-1} f(i,j) - \sum_{i=1}^{a-1} \sum_{j=1}^{b-1} f(i,j)$$

let $f(i,j) = \gamma^{k-i+l-j} \mathcal{K}_{p-1}^S(s'(1:i), t'(1:j))$, $a = k$ and $b = l$, we have:

Algorithm: *Recursive computation of the warped time resolved spectrum kernel.*

$$\mathcal{K}_p^{Sw}(k, l) = \mathcal{K}_{p-1}^S(s'(1:k), t'(1:l)) + \gamma \mathcal{K}_p^{Sw}(k, l-1)$$

$$+\gamma \mathcal{K}_p^{Sw}(k-1, l) - \gamma^2 \mathcal{K}_p^{Sw} \ (k-1, l-1) \quad (8)$$

$$\mathcal{K}_p^S(s'x, t'y) = \kappa^*(x, y)(x, y) \mathcal{K}_p^{Sw}(|s'|, |t'|)$$
$$\mathcal{K}_p(s'x, t') = \mathcal{K}_p(s', t') + \textstyle\sum_{j=1}^{|t'|} \mathcal{K}_p^S(s'x, t'(1:j))$$

$$\begin{aligned} \mathcal{K}_0^S(s', t') &= 1 \quad \textbf{for all } s', t', \\ \mathcal{K}_i^S(s', t') &= 0, \quad \textbf{if } \min(|s'|, |t'|) < i, \\ \mathcal{K}_i(s', t') &= 0, \quad \textbf{if } \min(|s'|, |t'|) < i, \end{aligned}$$

The computation of the kernel follows a dynamic programming technique with the order of $O(p|s||t|)$. We have recursions over the prefixes of the time series and the lengths of the subsequences and we do the routine above until $x = s_{|s|}$ and $|t'| = |t|$. As we see from the above pseudo-code, the evaluation of the $\mathcal{K}_i^{norm}$ is of order $O(|s||t|)$ and the overall complexity of our algorithm to calculate a linear combination of all p-spectrum kernels is $O(p|s||t|)$.

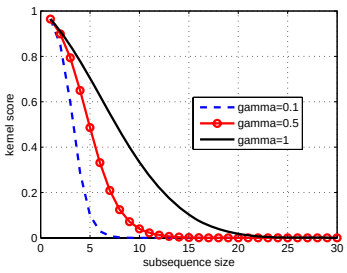

Fig. 6. Kernel score between two echoes of Ficus tree with different warping costs

Algorithm Warped Time resolved spectrum kernel

Input : Time series s and t of length n and m, max subsequence length l and warping cost γ;
Output: Array of spectrum kernel $\mathcal{K}[]$ with different sizes of subsequence-length from 1 to l);

$KPSw(0:n, 0:m) = 0$;
for $i \leftarrow 1$ **to** n **do**
  for $j \leftarrow 1$ **to** m **do**
    $KPS(i,j) = \kappa^*(s_i, t_j)$;
    $\mathcal{K}[1] = \mathcal{K}[1] + KPS(i,j)$;
  end
end
for $p \leftarrow 2$ **to** l **do**
  for $i \leftarrow 1$ **to** n **do**
    for $j \leftarrow 1$ **to** m **do**
      $KPSw(i,j) =$
      $KPS(i-1, j-1) + \gamma KPSw(i, j-1) +$
      $\gamma KPSw(i-1, j) - \gamma^2 KPSw(i-1, j-1)$;
      $KPS(i,j) = \kappa^*(s_i, t_j) KPSw(i-1, j-1)$;
      $\mathcal{K}[p] = \mathcal{K}[p] + KPS(i,j)$;
    end
  end
end
return $\mathcal{K}[]$

To prevent that with larger sizes of subsequences the kernel achieves a higher similarity score we normalize the kernel, $\mathcal{K}_i^{norm}(s,t) = \frac{\mathcal{K}_i(s,t)}{\sqrt{\mathcal{K}_i(s,s)\mathcal{K}_i(t,t)}}$. This operation scales the similarities in the range [0,1].

Fig. 6 plots the kernel score of two samples of echoes reflected by a Ficus tree with different values of warping cost. We see that as the gamma parameter gets closer to 1 we let subsequences of two time series warp more and the similarity score (kernel score) increases. When gamma is equal to zero, the kernel is equal to the time-resolved spectrum kernel [9].

In practice and especially in our classification task, it makes sense to consider the similarity of subsequences having different sizes and calculate a linear combination of different i-spectrum kernels with different weighting $\theta_i \geq 0$. The weighted kernel is:

$$K(s,t) = \sum_{i=1}^{p} \theta_i \mathcal{K}_i^{norm}(s,t) \qquad (9)$$

B. Optimal kernel selection

Finding suitable values of the parameters θ_i in Eq. 9 is a case of more general problem known as optimal kernel selection. For this task we selected the optimal kernels via maximizing the Kernel Fisher Discriminant (KFD) criterion [10] through the method of Kim et. al [11]. In their method the task is considered as a convex optimization problem and the objective function (KFD) is converted to the shape of standard form of Semi Definite Programming (SDP) (interior point method). To solve this optimization problem we used the SDP solver of SeDuMi [12].

IV. Experiment and Results

We gathered the sonar data, 720 echoes for each tree shown in (Fig. 3). After the preprocessing steps for each echo (Fig. 4), we have a time series in which each point is a time frame and its value is an array of the average energy of each channel of gammatone filter. We selected randomly 100 echoes of each tree and then calculated $\mathcal{K}_i^{norm}(s[m], s[n])$ for $i \in [1, l]$, $m, n \in [1, 100]$ and $\sigma(Eq.5) \in \{1, 10, 100, 1000\}$ where $s[m]$ and $s[n]$ are the m-th and n-th of pre-processed echoes and l is the length of the time series (in our experiment 90). Using the optimal kernel selection noted above, we found the optimal value for θ_i in Eq. 9 and calculated the matrix K:

$$\mathbf{K}(i,j) = K(s[i], s[j]) = \sum_{k=1}^{l} \theta_i^{opt} \mathcal{K}_l^{norm}(s[i], s[j])$$

in which $i, j \in [1, 300]$ and $s[i]$ is i-th echo, for Ficus echoes $i \in$[1,100], for Bamboo $i \in$ [101,200] and for Schefflera $i \in$[201,300]. In this study, we found that suitable value for σ (Eq. 5) is in the range [10,100].

A SVM learns a classification function $f(x)$ of the form:

$$f(x) = \sum_{i; x_i \in \chi_+} \lambda_i K(x, x_i) - \sum_{i; x_i \in \chi_-} \lambda_i K(x, x_i) \qquad (10)$$

where non-negative λ_i weights are computed during training by maximizing a quadratic objective function and $K(.,.)$ is the kernel. Given this function, a new data x is predicted to belong to the positive dataset, if the value of $f(x)$ is positive, otherwise it belongs to the negative dataset. After training the classifier, we used the remaining data (1860 echoes) for testing.

Figure 7 shows the accuracy of the classifier for those trees with different warping costs (γ) and $\sigma = 100$, based on the number of echoes as observation. It shows a high accuracy even for a low number of echoes. We see that

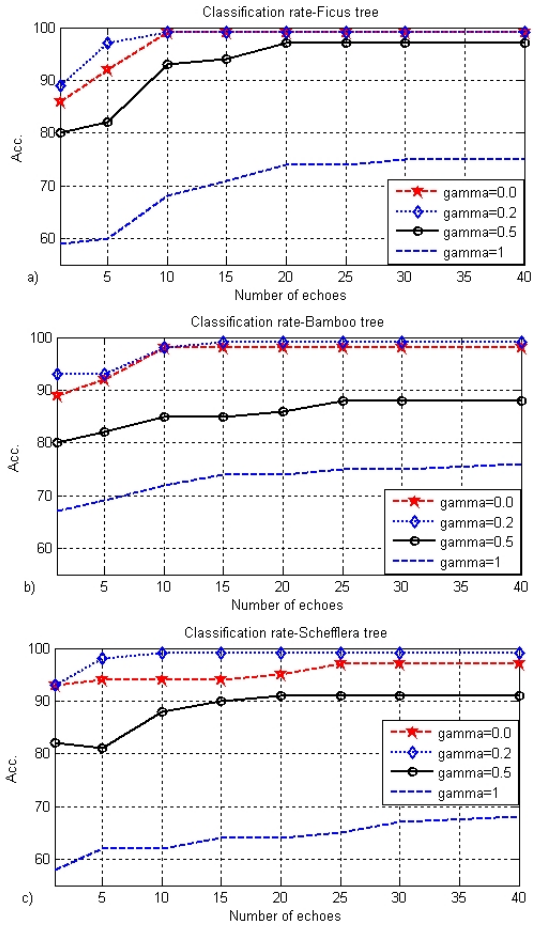

Fig. 7. The accuracy of the classifier using our suggested kernel with different warping costs ($\sigma = 100$) for a) ficus, b) Bamboo and c)Schefflera. When $\gamma = 0$ the kernel is similar to time-resolved spectrum kernel [9].

the parameter γ can affect the accuracy of the classifier and the accuracy of the time-resolved spectrum kernel [9] increases in each tree by changing the parameter γ. Table 1 shows the accuracy of classifier when it decides based on only one observation. Best accuracy for Ficus, Bamboo and Schefflera trees are gained for $\gamma = 0.1$, $\gamma = 0.3$ and $\gamma = 0.2$, respectively. This parameter lets the kernel to consider a warping (with a cost) for the subsequences of the time series and extract their similarity. Considering that parameter in our classification task is justifiable, because the echoes reflected by the adjacent leaves of each tree can have somehow similar patterns but not exactly the same, so we need to have a parameter (γ) that can let the kernel capture those similarities, too. The optimal value of that parameter for each tree can be related to the physical specification of each tree. As we see if the γ gets closer to 1 (no cost for warping) the accuracy decreases.

Comparing with the previous works of our group (Wang et al. [7]), it shows a notable improvement in accuracy. The best result for classification gained before was through template matching in 2D biosonar acoustic images (using a 2D Discrete Cosine Transform). The classification was made

γ	Ficuss	Bamboo	Schefflera
$\gamma = 0$	86.2	89.5	90.2
$\gamma = 0.1$	**89.1**	90.1	91.3
$\gamma = 0.2$	88.6	91.4	**93.8**
$\gamma = 0.3$	87.6	**93,1**	91,1
$\gamma = 0.5$	80.1	81.3	82.1
$\gamma = 0.1$	59.2	67.4	58.1

TABLE I

CLASSIFICATION RATE BASED ON DIFFERENT VALUES OF γ

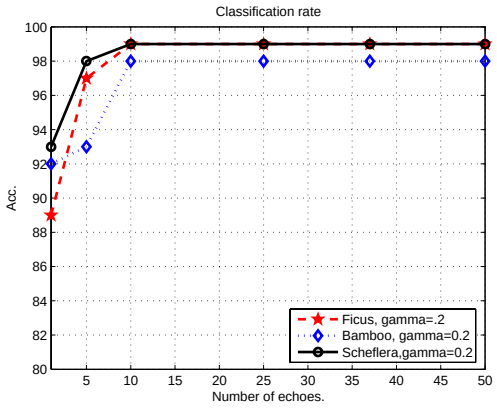

Fig. 8. The accuracy of classifiers using different numbers of echoes for testing with the Warped Time-resolved spectrum kernel ($\gamma = 0.2$).

via extracting the maximum normalized cross correlation between the acoustic templates (Fig. 9). As shown in Fig. 8, we could get higher accuracy in both single and repeated observations (even with fewer echoes) compared with Fig. 9 (note the different horizontal and vertical axes).

V. ACKNOWLEDGMENT

We would like to thank Maosen Wang for the preparation of the biosonar based robot. The biosonar head we used was built according to a design of Dr. Rolf Müller in the neurobiology lab of Prof. Dr. H.-U. Schnitzler, university of Tübingen, in a former joint research project.

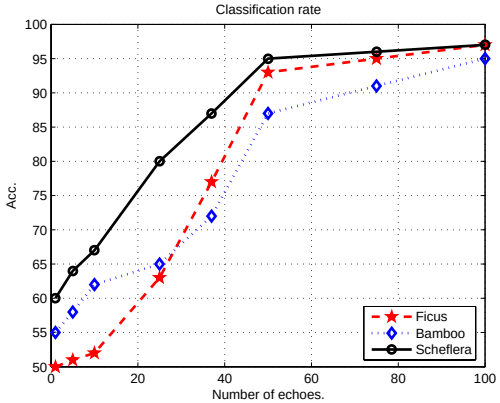

Fig. 9. The accuracy of classifier via Template matching using acoustic images of echoes (Wang et al. [8]).

REFERENCES

[1] J. -E. Grunwald, S. Schörnich and L. Wiegrebe , "Classification of natural textures in echolocation", *in Proc. Natl. Acad. Sci. USA.*, vol. 101, pp. 5670-5674, 2004

[2] D. Ratner and P. McKerrow , "Landmark recognition with CTFM ultrasonic sensing", *in Proc. ACRA 2001.*, pp. 104-110, 2001

[3] R. Muller, "A computational theory for the classification of natural biosonar targets based on a spike code", *in Network: Computat. Neural Syst.*, vol. 14, pp. 595-612, 2003

[4] R. Kuc, "Transforming echoes into pseudo-action potentials for classifying plants", *in J. Acoust. Soc. AM.*, vol. 110, pp. 2198-2206, 2001

[5] J. A. Simmons, N. Neretti, N. Intrator, R. A. Altes and M. J. Ferragamo, "Delay accuracy in bat sonar is related to the reciprocal of normalized echo bandwidth, or Q", *in Proc. Natl. Acad. Sci. USA.*, vol. 101, pp. 3638-3643, March 2004.

[6] W. Gao and Mark Hinders, "Mobile Robot Sonar Backscatter Algorithm for Automatically Distinguishing Walls, Fences, and Hedges.", *in The International Journal of Robotics Research*, vol. 25(2), pp. 135-145, 2006.

[7] M. Wang and A. Zell, "Classification of natural landmarks with Biosonar", *in Journal of the Acoustic Society of America (JASA)*, vol. 116, 2004.

[8] M. Wang, "Natural Landmark Classification with a Biosonar based Mobile Robot", *PhD thesis, University of Tübingen*, 2006.

[9] M M. Beigi, M. Wang and A. Zell, "Time-resolved spectrum kernel for biosanar target classification", *in Signal Processing, Pattern Recognition, and Applications*, February 2007, to be published.

[10] S. Mika, G. Rätsch, J.Weston, B. Schölkopf, and K.-R. Müller, "Fisher discriminant analysis with kernels". *In Y.-H. Hu, J. Larsen, E. Wilson, and S. Douglas, editors, Neural Networks for Signal Processing IX*, pp. 41-48. IEEE, 1999.

[11] S.-J. Kim, A. Magnani and S. Boyd, "Optimal Kernel Selection in Kernel Fisher Discriminant Analysis", *in Proceeding of the 23th Int. Conf. on Machine Learning (ICML)*, pp. 465-472,2006.

[12] J. Strum, "Using SeDuMi 1.02, a Matlab toolbox for optimization over symmetric cones",Available from `sedumi.macmaster.ca/`.